Modulations in Spectra of Galactic Gamma-ray sources as a result of photon-ALPs mixing.

Jhilik Majumdar[1], Francesca Calore[2], Dieter Horns[1]

27.07.17

[1] Institute for Experimental Physics, University of Hamburg.
[2] Laboratoire d'Annecy-le-Vieux de Physique Théorique, CNRS

Universität Hamburg
DER FORSCHUNG | DER LEHRE | DER BILDUNG

Introduction

CP violation in QCD: Axion intoduced

Most general gauge invariant Lagrangian of QCD:

$$L = -\frac{1}{4} G^a_{\mu\nu} G^{a,\mu\nu} + \overline{q}(i\gamma_\mu D^\mu - M_q) - \frac{\alpha_s}{8\pi}\theta G^a_{\mu\nu}\tilde{G}^{a,\mu\nu} \quad (1)$$

Topological theta term $\propto G^a_{\mu\nu}\tilde{G}^{a,\mu\nu} \propto E^a.B^a$ violates CP.

Clear indication from : electric dipole moment of neutron ($d_n \sim 6 \times 10^{-17}\theta ecm$).

Experimental value $\Rightarrow \mid \theta \mid < 10^{-9}$

Solve to CP problem: Pseudo-scalar particle Axion comes.

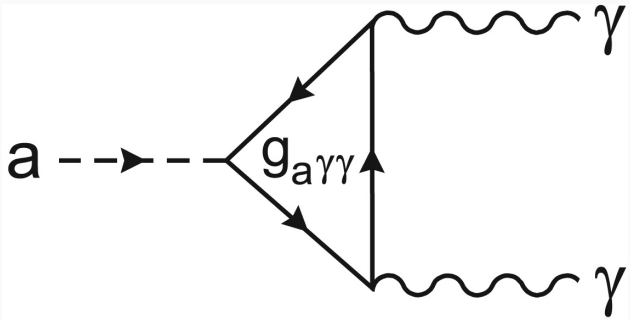

Figure 1: Y. Semertzidis et. al,2015.

ALPs have the property:

Oscillate into photons or vice-versa in the presence of magnetic field.

Current Axion limits:

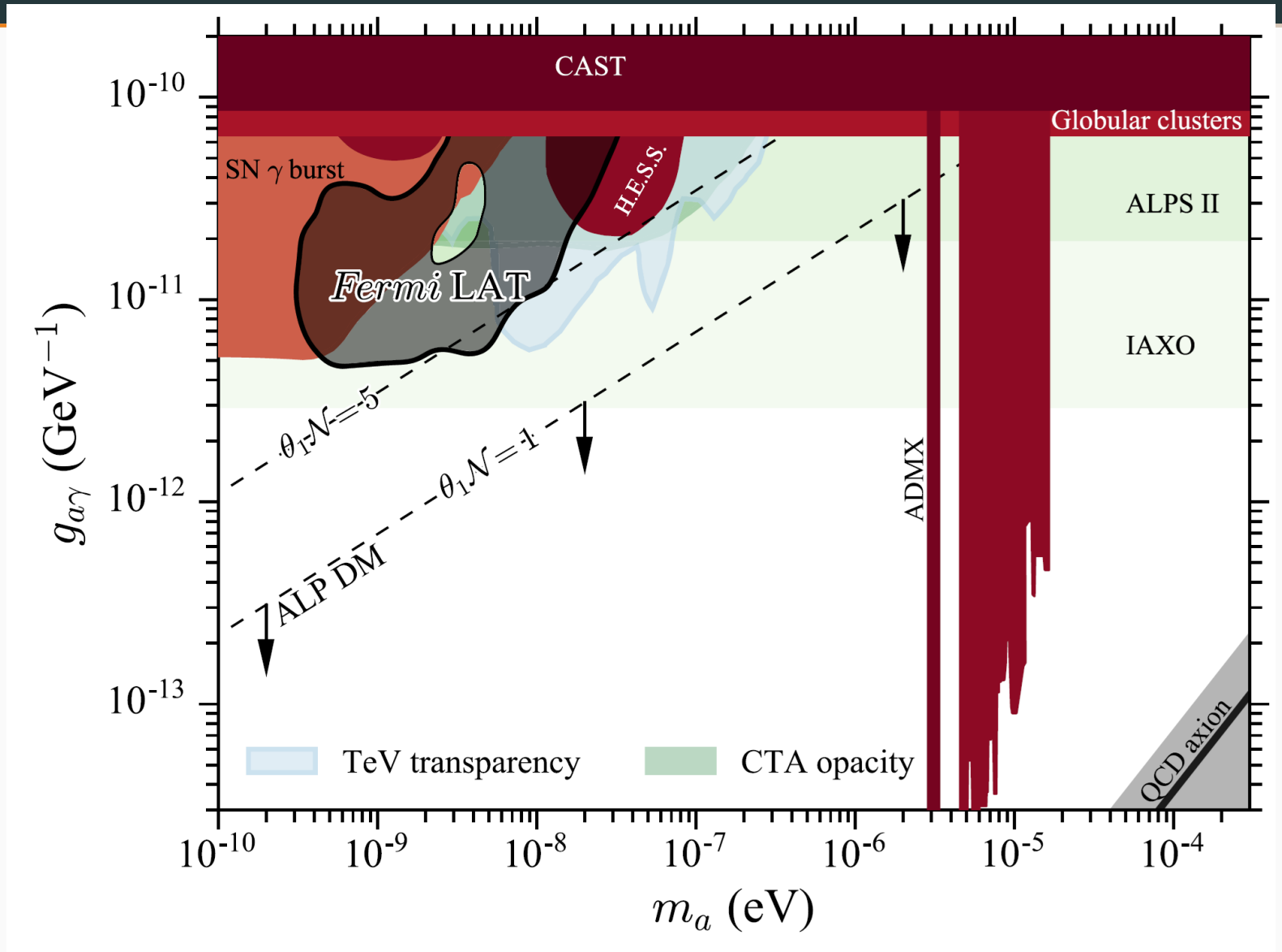

Figure 2: Parameter space for axions and axion-like particles [M. Meyer et al. 2016].

Spectral distortion due to Photon-ALPs mixing:

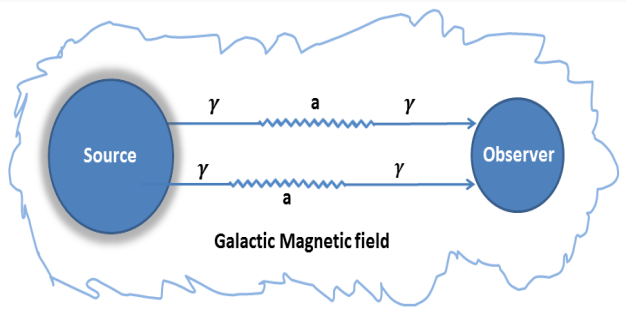

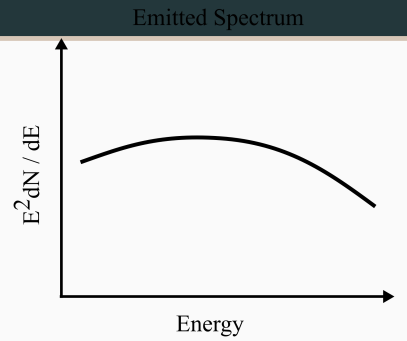

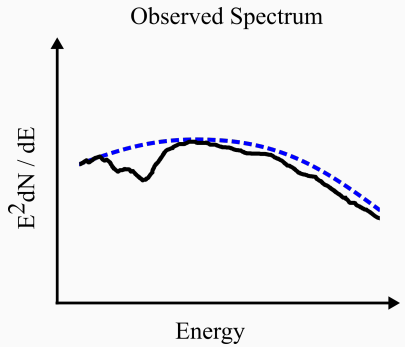

The probability of the conversion in a distance of 0 to d is :

$$P_{\gamma\to a} = \frac{g_{\alpha\gamma}^2}{8}\left(\left|\int_0^d dz' e^{2\pi i z'/l_0} B_x(x,y,z')\right|^2 + \left|\int_0^d dz' e^{2\pi i z'/l_0} B_y(x,y,z')\right|^2\right) \quad ; g_{\alpha\gamma} Bd \ll 1 \qquad (2)$$

where, $B_t = \sqrt{B_x^2 + B_y^2}$ and $l_0 = 4\pi E/m_a^2$. [Mirizzi et al. 2007]

$g_{\alpha\gamma}$:a coupling constant of dimension $(energy)^{-1}$

Observations:

Detecting gamma rays with Fermi LAT

- Gamma ray space telescope.
- Field of view : 20% of sky at a time.
- Effective area: $1m^2$.
- Energy range from about 100 MeV to more than 500 GeV.
- Orbital period: 1.6 hours.
- Point spread finction: 0.8° at 1 GeV.

Figure 3: Fermi Large Area Telescope[Image Credit: NASA/Fermi LAT Collaboration]

Source selection:

Source selection criterion:

- Bright Galactic sources.
- Sources that are crossing the spiral arms along the line of sight.

Pulsar list:

1. J2021+3651
2. J1420-6048
3. J2240+5831
4. J1648-4611
5. J1718-3825
6. J1702-4182

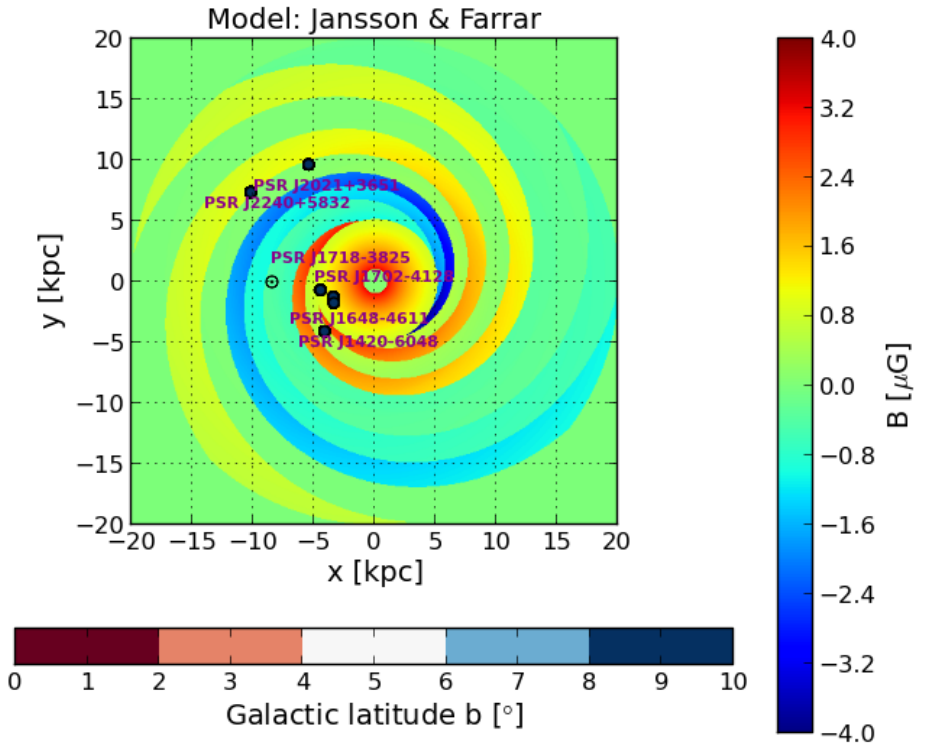

Figure 4: Source positions in the plane of Galactic magnetic field(Jansson & Farrar model; Jansson et al. 2012).

Data Analysis:

Fermi-LAT data analysis:

- 8 years of Fermi LAT data Pass 8 data [Ackermann et al. 2014].
- ENRICO binned likelihood(i.e. Fermi gtlike) optimization(Sanchez & Deil, 2013) technique has been performed.
- Energy region: 100 MeV to 300 GeV.
- Energy bins: 25.
- Pulsar spectrum is modelled by a power law with exponential cutoff:

$$\frac{dN}{dE} = N_0 \left(\frac{E}{E_0}\right)^{-\Gamma} exp\left(-\frac{E}{E_{cut}}\right) \tag{3}$$

Fermi-LAT data analysis:

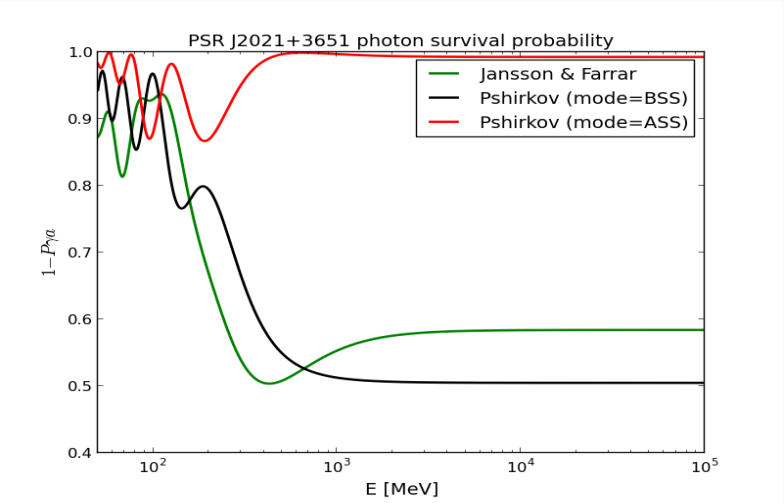

Figure 5: The conversion probability of the photon to axion as a function of energy.

$$\left(\frac{dN}{dE}\right)_{bin} = \left(1 - P_{\gamma \to a}\left(E, g_{a\gamma}, m_a\right)\right) \cdot \left(\frac{dN}{dE}\right)_{model,bin} \quad (4)$$

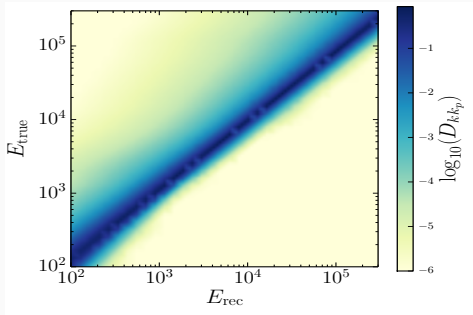

Figure 6: Energy dispersion matrix.

- We perform a fit to the data, minimising the χ^2 function.
- Log(likelihood) has a parabolic pattern.
- Energy dispersion matrix derived for all the EDISP event types together.

Fermi-LAT data analysis:

- For P8R2 SOURCE V6 event class, systematic uncertainties in effective area are derived to be about 2.4 %.

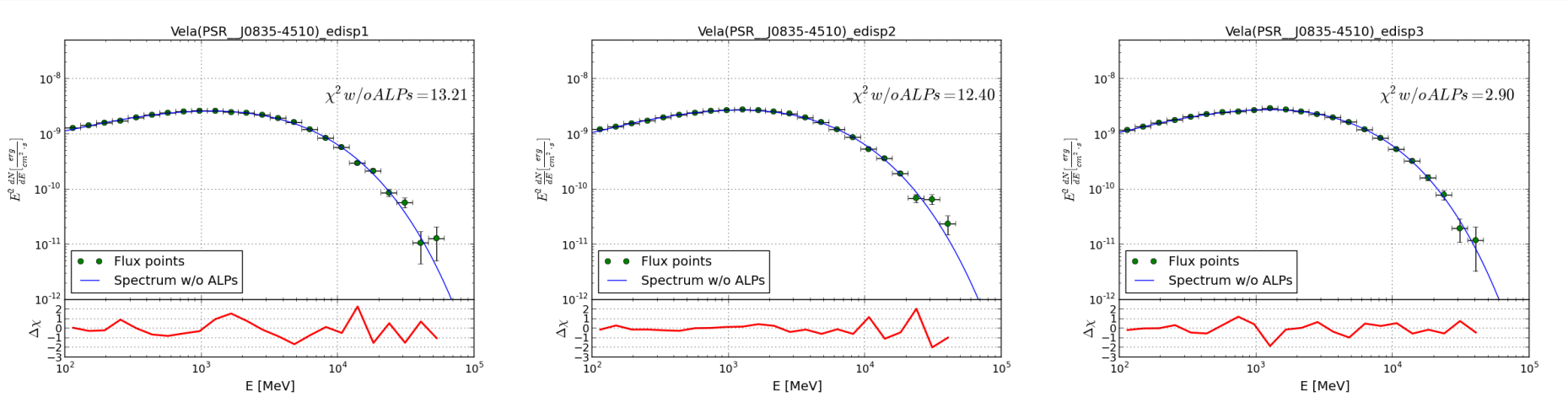

Figure 7: Systematic uncertainties of Vela Pulsar for EDISP1, EDISP2, EDISP3 event types.

- Signature of photon-ALPs oscillations, including the effect of oscillations in the predicted spectra:

$$\left(\frac{dN}{dE}\right)_{fit} = D_{kk_p} . (1 - P_{\gamma \to a}(E, g_{a\gamma}, m_a)) . \left(\frac{dN}{dE}\right)_{model} \qquad (5)$$

Results:

Pulsar spectrum:

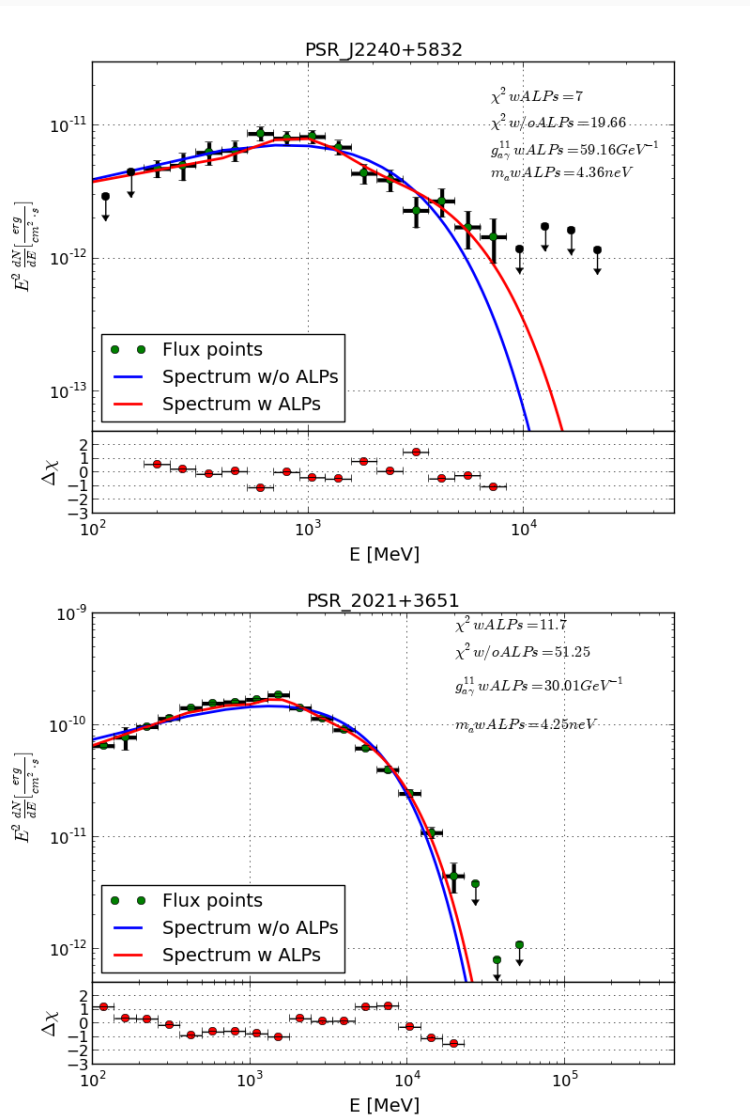

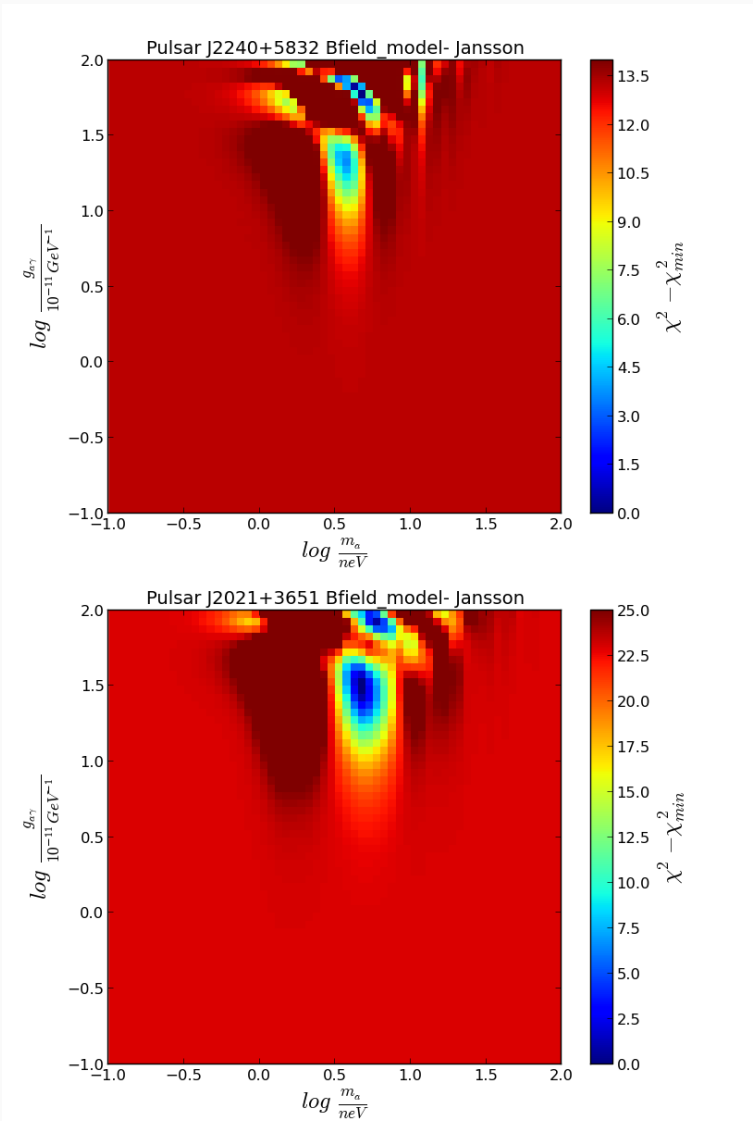

Figure 8: Best-fit model of the spectrum of Pulsar candidates. Right panel: The χ^2 scan as function of photon-ALPs coupling and ALPs mass.

Pulsar spectrum:

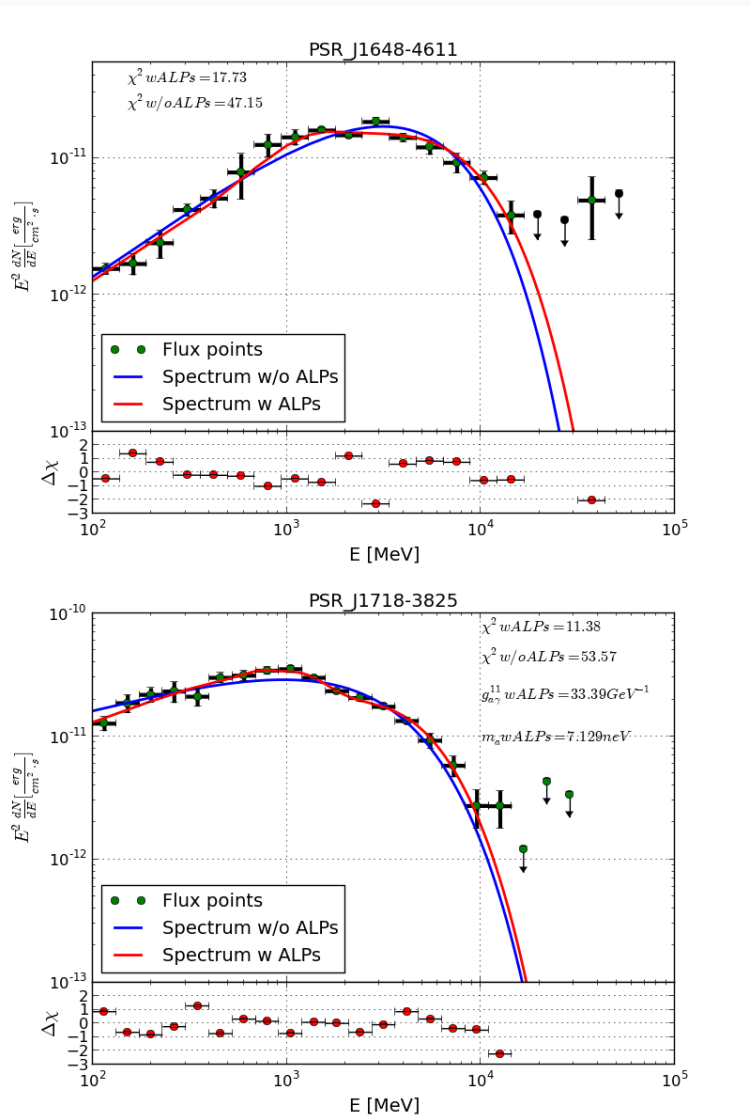

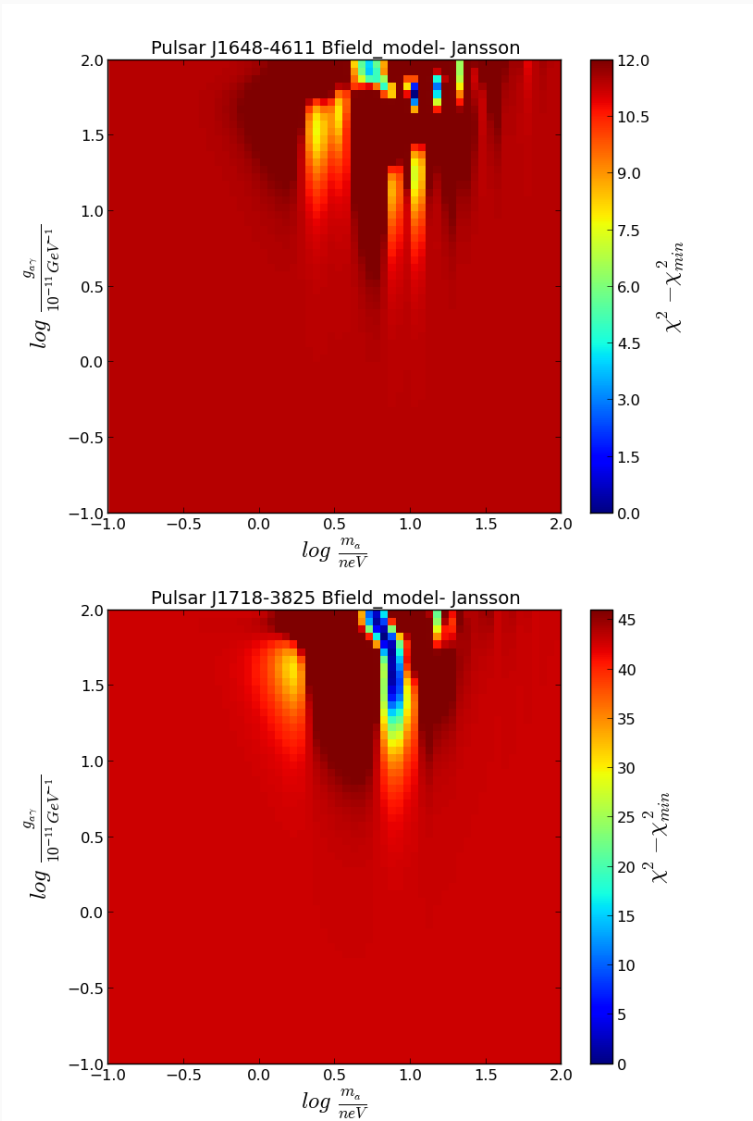

Figure 9: Best-fit model of the spectrum of Pulsar candidates. Right panel: The χ^2 scan as function of photon-ALPs coupling and ALPs mass.

Combined Photon-ALPs coupling and ALPs mass sensitivity:

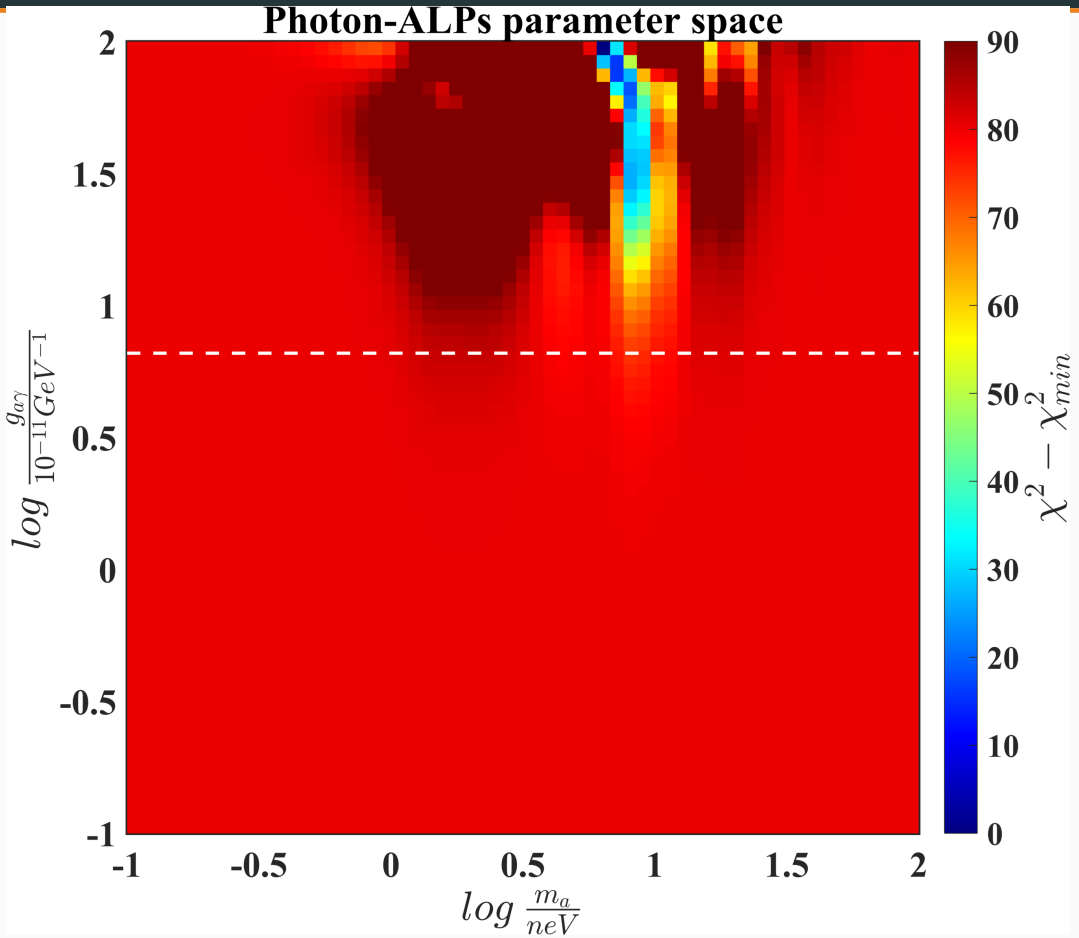

Figure 10: combined χ^2 scan as function of photon-ALPs coupling and ALPs mass.

Significance level estimated by F-test: 7.5σ.

Conclusion:

Summary:

- Indications for ALPs in case of Fermi LAT data of **galactic pulsar candidate**.
- Photon-ALPs mixing is non-linear in the spiral arms and in the large scale field of the inner Galaxy.
- ALPs mass bounds: 5 neV$\leq m_a \leq$ 8 neV
- Photon-ALPs coupling bound: 20 - 80 $\times 10^{-11} GeV^{-1}$
- Significance level : 7.5σ.
- The main challenge of this work is to choose the magnetic field model as the resulting mixing parameters are quite model dependent.

Thank you!

Backup slides

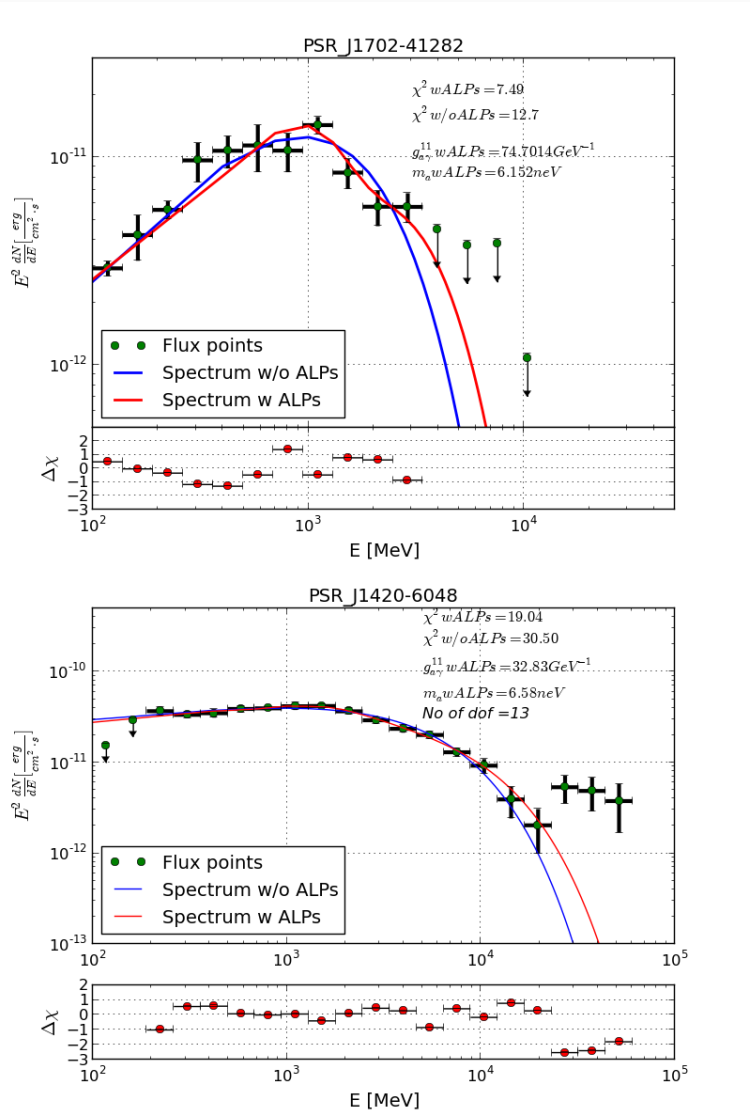

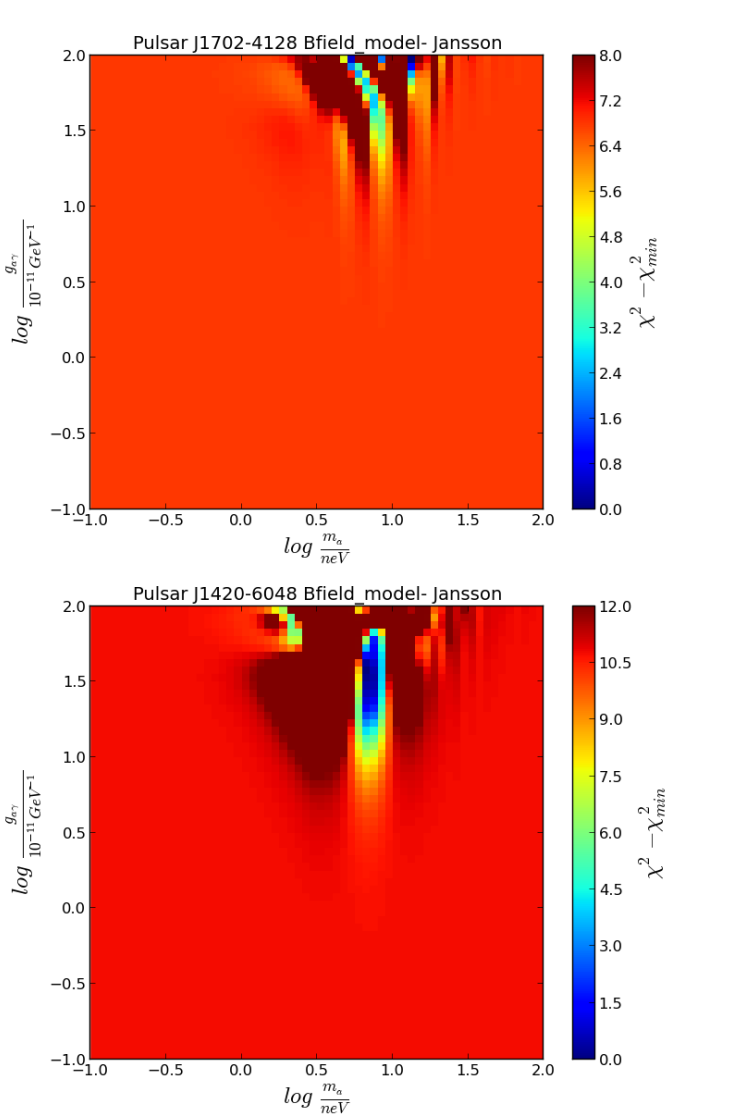

Figure 11: Best-fit model of the spectrum of Pulsar candidates. Right panel: The χ^2 scan as function of photon-ALPs coupling and ALPs mass.

back up slides

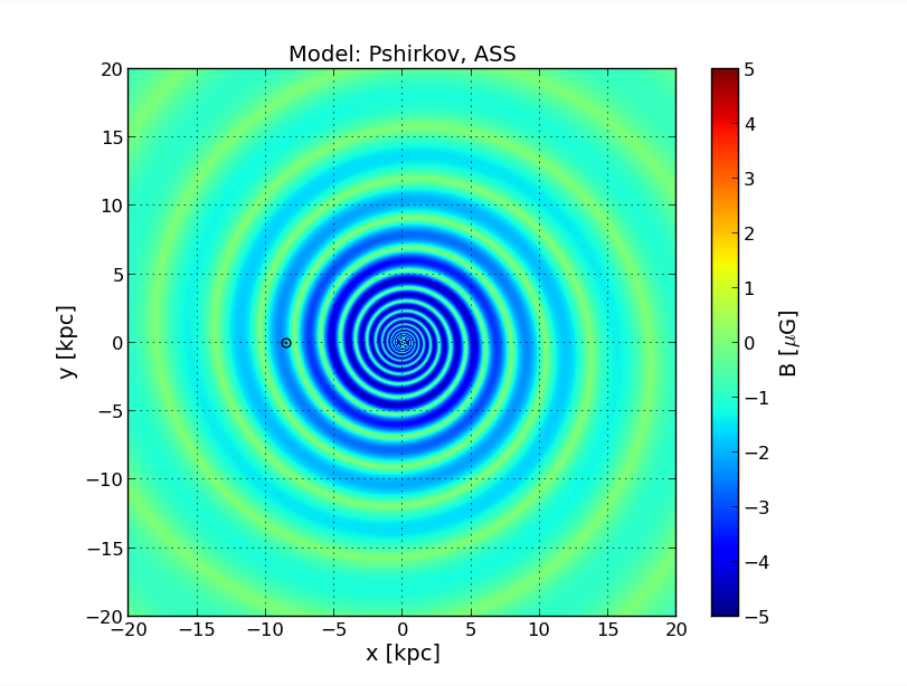

Figure 12: Bfield model: Pshirkov ASS model

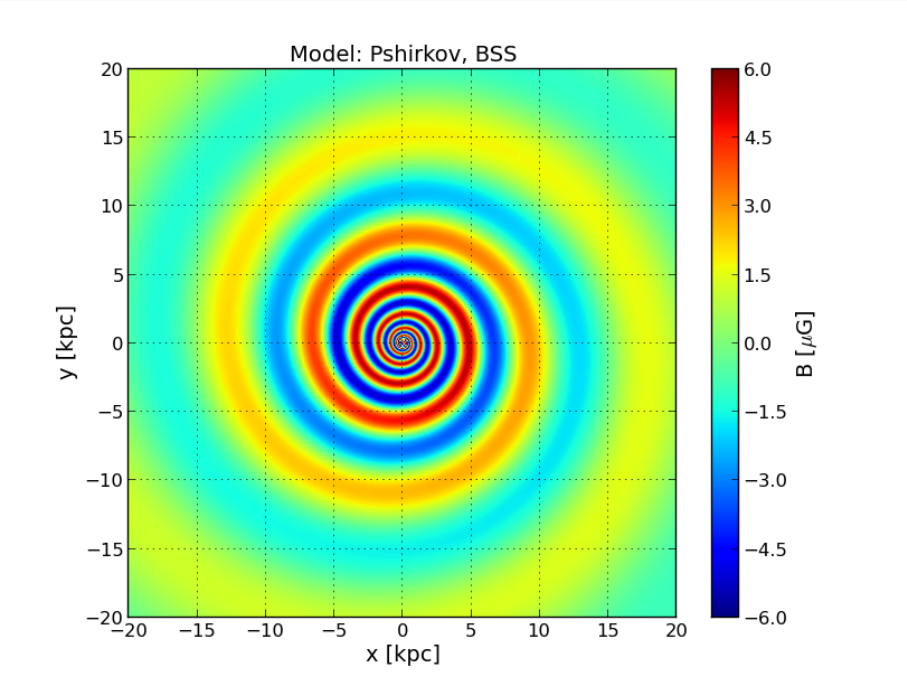

Figure 13: Bfield model: Pshirkov BSS model

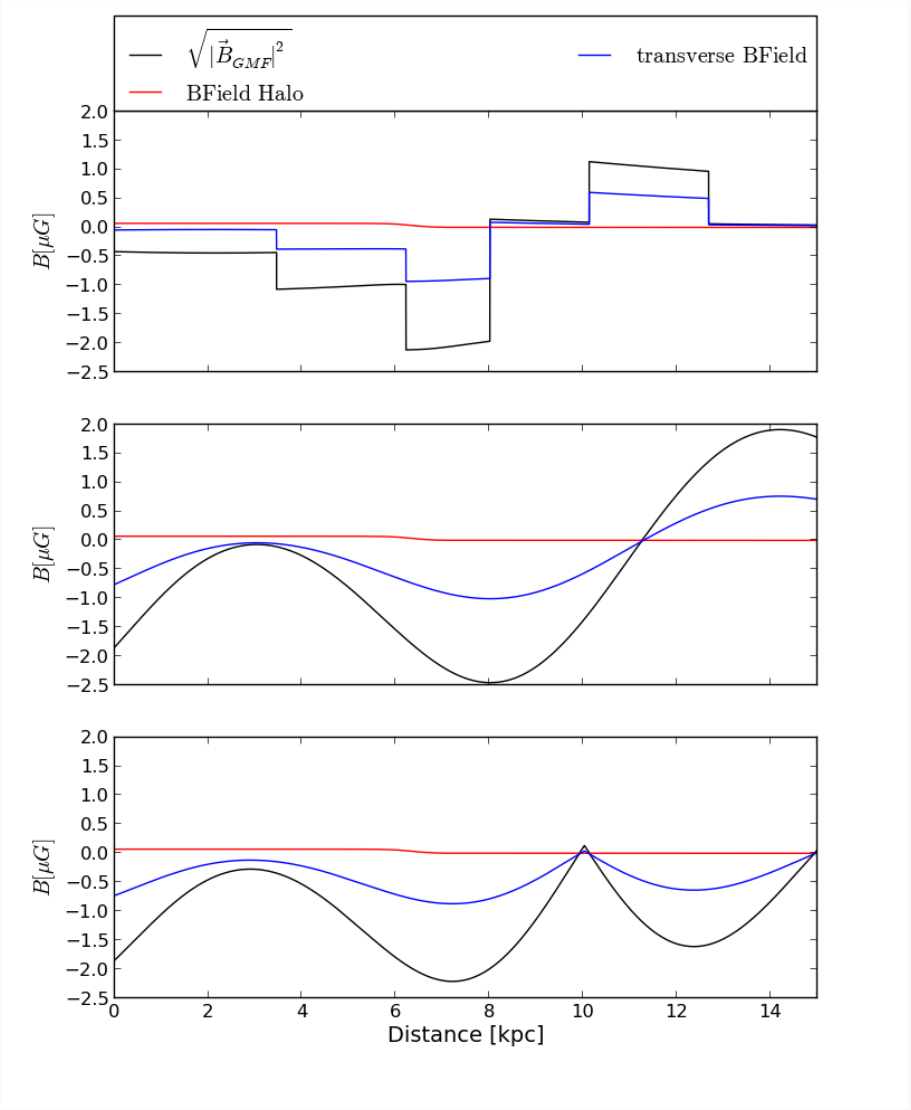

Figure 14: Bfield model:Magnetic field along the line of sight of the pulsar J2021 +3651.Top panel for the model of Jansson-Farrar, middle panel for the model of Pshirkov in BSS, bottom in ASS mode.

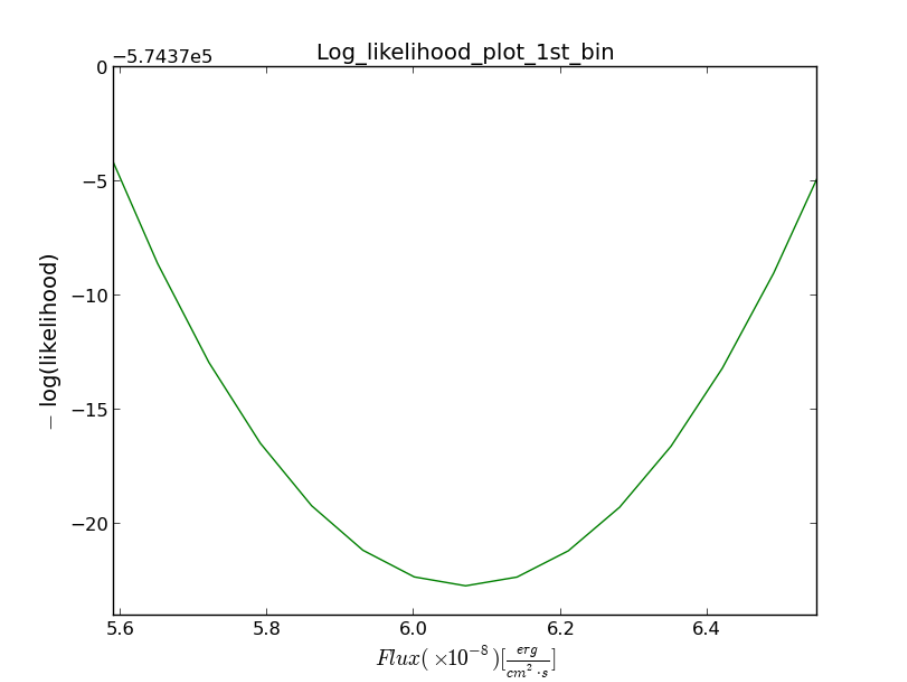

Figure 15: Log-likelihood as a function of flux for first energy bin of PSR J2021+3651.

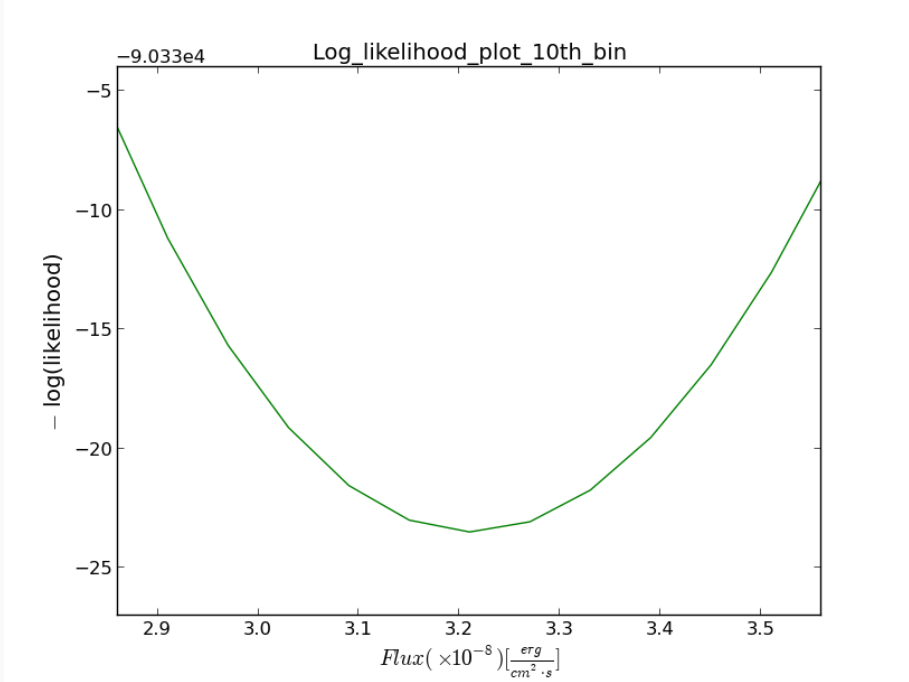

Figure 16: Log-likelihood as a function of flux for 10th energy bin of PSR J2021+3651.

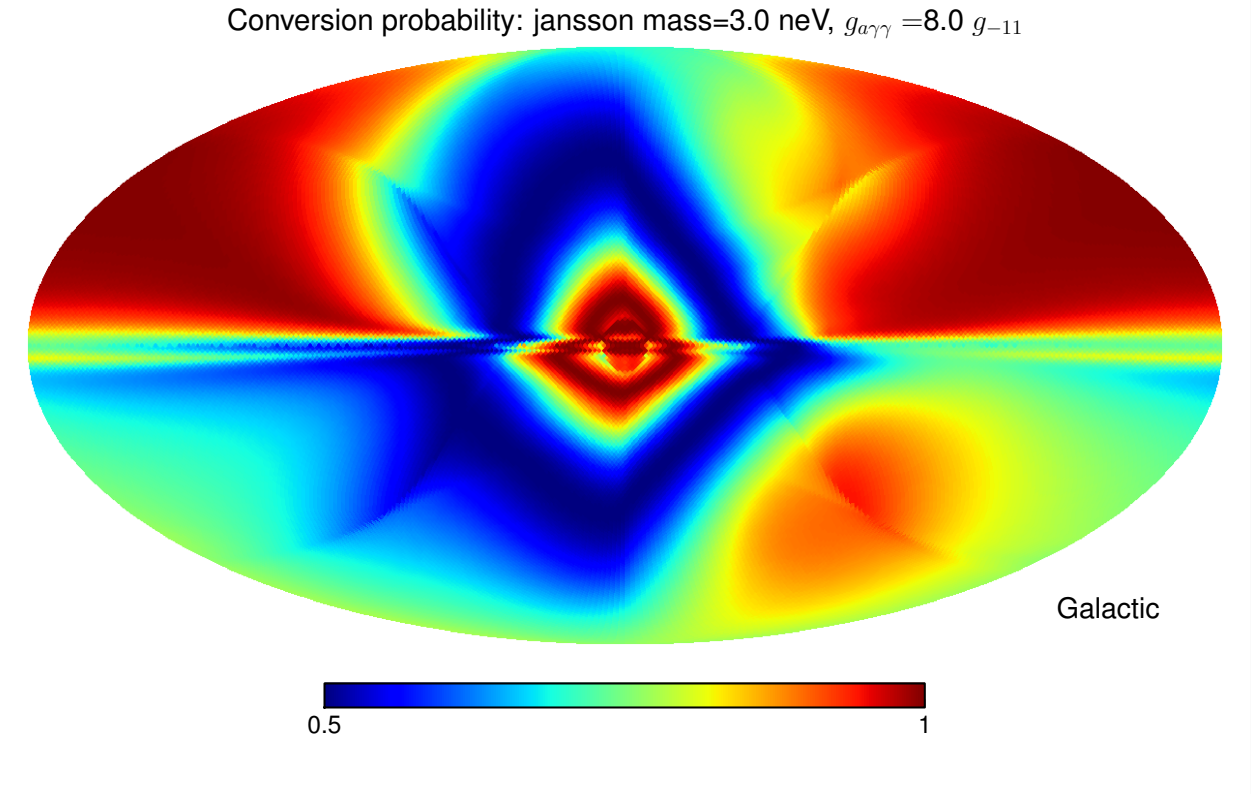

Figure 17: Conversion probability of photon to axion in allsky map.